Analytica Chimica Acta 1128 (2020) 203–210

Contents lists available at ScienceDirect

Analytica Chimica Acta

journal homepage: www.elsevier.com/locate/aca

# Screening and application of a truncated aptamer for high-sensitive fluorescent detection of metronidazole

Hao Wei , Rongfeng Cai , Hui Yue , Yaping Tian , Nandi Zhou *

*The Key Laboratory of Carbohydrate Chemistry and Biotechnology, Ministry of Education, School of Biotechnology, Jiangnan University, Wuxi, 214122, China*

## HIGHLIGHTS

- A metronidazole aptamer was obtained via library-immobilized SELEX and truncation.
- Fluorescent detection of metronidazole was established using the truncated aptamer.
- The assay exhibited high sensitivity and good practicability.

## GRAPHICAL ABSTRACT

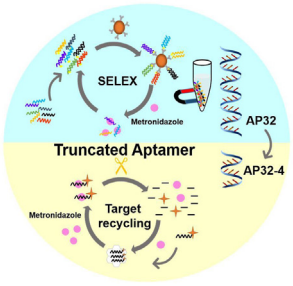


## ARTICLE INFO

*Article history:*
Received 10 February 2020
Received in revised form
27 June 2020
Accepted 1 July 2020
Available online 17 July 2020

*Keywords:*
Magnetic beads SELEX
Aptamer
Fluorescent biosensor
Target-recycling signal amplification
Metronidazole

## ABSTRACT

Aptamer-based biosensors have been widely constructed and applied to detect diverse targets. Metronidazole is a widely used broad-spectrum antibacterial drug, whose residue has multiple risks to human health. Herein, metronidazole-specific aptamers were selected from a random ssDNA library with the full length of 79 nucleotides (nt) based on DNA library-immobilized magnetic beads SELEX technology. After ten rounds of selection, four aptamers with highly similar secondary structures were selected, among which AP32, with the lowest dissociation constants, was chosen as the optimal aptamer for further optimization. Then a semi-rational post-SELEX truncation was carried out based on the secondary structure analysis and molecular docking, as well as affinity assessment. Redundant nucleotides in AP32 were stepwise removed without the decrease of affinity. Following such strategy, a truncated aptamer AP32-4 with the length of only 15 nt was eventually screened. The dissociation constant of 77.22 ± 11.27 nM is almost equivalent to the original AP32. Furthermore, an aptamer-based fluorescent biosensor for metronidazole was constructed based on AP32-4. With the help of exonuclease-assisted target-recycling amplification, the biosensor exhibits a linear detection range of 25–800 nM, and the detection limit of 10.50 nM. The biosensor was applied to detect metronidazole in honey samples. The results show that not only an efficient strategy for screening robust and practicable aptamers, but also an ultrahigh sensitive detection platform for metronidazole were established.



## 1. Introduction

Metronidazole [1-(2-hydroxyethyl)-2-methyl-5-nitroimidazole] is a synthetic nitroimidazole derivative which has been widely used in human and veterinary medicine due to its broad-spectrum

* Corresponding author.
*E-mail address:* zhounandi@jiangnan.edu.cn (N. Zhou).

https://doi.org/10.1016/j.aca.2020.07.003
0003-2670/

antibacterial and antiprotozoal activity [1]. Metronidazole (MNZ) used to be added to feed to prevent infection and promote weight gain [2]. It was even reported to be illegally added to cosmetic materials to reduce skin infection [3]. However, studies have shown that improper use of metronidazole has potential risks of teratogenicity, carcinogenicity and nerve mutagenesis [4]. Therefore, it is important to achieve high-sensitive and high-specific quantitative determination of metronidazole. Conventional methods for metronidazole detection include spectrophotometry [5], high-performance liquid chromatography [6], fluorescence [7], UV spectrophotometry [8], gas chromatography [9] and ion mobility spectrometry [10]. These methods require either advanced equipment and professional technical personnel, or high cost and complicated sample processing. Biosensors with high-specific recognition elements and efficient signal amplification offer accurate and rapid detection for diverse targets. However, the lacking of specific recognition elements greatly restricts the application of biosensing technique in metronidazole detection. Although several biosensors for metronidazole have been reported, they generally employed molecularly imprinted polymer or nanomaterials as recognition elements [11–13]. Immunosensor for metronidazole has been reported [14], yet the high quality antibody of metronidazole is still not available. Therefore, it is necessary to screen novel recognition elements and establish accurate, sensitive and rapid detection of metronidazole.

Since the emergence of systematic evolution of ligands by exponential enrichment (SELEX) technology, various aptamers for different targets have been selected and applied in diverse areas including the construction of aptamer-based biosensors. With the continuous development of SELEX technology, new materials and strategies have been employed in SELEX process, particularly for small molecules, such as capillary electrophoresis (CE)-SELEX [15], graphene oxide (GO)-SELEX [16], multi-GO-SELEX [17] and capture-SELEX [18]. Nevertheless, magnetic separation-based SELEX is still regarded as the most efficient way to select aptamers from random ssDNA pool. The use of magnetic beads and external magnets allows relatively fast, simple and gentle separation of various molecules in different lower volume matrices [19,20]. Previously we successfully obtained several antibiotics-specific aptamers by employing the conventional target-immobilized magnetic beads-based SELEX [21,22]. To immobilize DNA library onto the magnetic beads further improves the magnetic beads-based SELEX. By using a 5′-biotinylated primer during PCR amplification, dsDNA in PCR products can be immobilized onto streptavidin-modified magnetic beads. Then targets replace those ssDNA with affinity from dsDNA on the beads through competitive binding. DNA library-immobilized SELEX has apparent advantages over target-immobilized SELEX. On one hand, important characterized functional groups of targets may be consumed during immobilization, which reduces the binding sites of the aptamers. On the other hand, only ssDNA with high affinity for targets will be recovered during DNA library-immobilized SELEX, because the competitive binding of ssDNA to targets requires the higher affinity of ssDNA for targets than their complementary sequences. This means the higher efficiency of the selection.

Post-SELEX optimization is a critical step to obtain real practical aptamers with reliable affinity and low cost. It is also the reason that only several so-called “star aptamers” have been frequently used to construct diverse aptasensors. Aptamer truncation can effectively reduce the synthetic cost and improve the application value of aptamers through cutting off unnecessary segments within the ssDNA sequences [23–26]. For example, the fixed sequences flanked at both sides of the random sequences in building ssDNA library, which are used as primer binding regions in PCR and accounting for about 50% of the total length, are sometimes proven not conducive to the overall structures of aptamers and can therefore be truncated. On the contrary, sequences with good homology can be persisted for further binding analysis. Appropriate truncation can be carried out based on structural analysis and binding sites prediction until the shortest aptamer sequences are found [27,28].

In this work, DNA library-immobilized SELEX was employed to select metronidazole-specific aptamers. After ten rounds of selection, four aptamers with highly similar secondary structures were selected, among which the one with the highest affinity, AP32 was chosen for post-SELEX truncation. The truncated aptamer has a greatly reduced length of the sequence with almost unchanged affinity. After the characterization of the truncated aptamer, it was considered to build a simple and efficient biosensor to evaluate its performance in practical detection. Graphene oxide (GO) has been widely used in both SELEX process and construction of aptamer-based biosensors, due to its stronger adsorption of ssDNA than dsDNA or DNA/target complexes [29–32]. This strategy can be more efficient in case a short-length ssDNA is employed, since the adsorption of short aptamers on the surface of GO is comparatively weak and the formation of the aptamer/target complexes is more reliable. Meanwhile, to increase the sensitivity of the detection, target-recycling strategy was frequently employed [33–36]. Thus a simple, highly sensitive and specific target-recycling fluorescence assay based on the truncated aptamer was designed for the detection of metronidazole.

## 2. Experimental

### 2.1. Aptamer selection

DNA library-immobilized SELEX was carried out. The initial random ssDNA library was firstly amplified by PCR with a pair of FAM-labeled forward primer and biotinylated reverse primer. The PCR product, dsDNA was immobilized on the surface of streptavidin-modified magnetic beads through the strong interaction between biotin and streptavidin. When the dsDNA-immobilized beads were incubated with the target metronidazole, the single-stranded sequences possessing the higher affinity towards the target than their complementary sequences formed ssDNA/metronidazole complexes and were released from the beads. After magnetic separation, the beads were removed and the ssDNA sequences in the solution were determined by fluorescent analysis, and used as the secondary library for further PCR amplification. Such selection was continuously performed for several rounds until the fluorescence intensity of the released ssDNA reached saturation. As the number of selection rounds increased, ssDNA sequences with the higher affinity for metronidazole were gradually enriched, while those with lower affinity were gradually eliminated (Fig. 1A).

To keep the magnetic beads active, streptavidin-modified magnetic beads were washed 5 times with PBS buffer (137 mM NaCl, 2.7 mM KCl, 4.3 mM $Na_2HPO_4$ and 1.4 mM $KH_2PO_4$, pH 8.0). In the first selection round, the initial ssDNA library was amplified by PCR (Material and method are detailed in the Supporting information). 200 μL PCR product was mixed with 200 μL binding buffer (50 mM Tris-HCl containing 5 mM KCl, 100 mM NaCl and 1 mM $MgCl_2$, pH 7.4). Then 80 μL streptavidin-modified magnetic beads were added and the mixture was gently shaken for 2 h at room temperature. With the help of a magnetic separator, the supernatant was removed. The magnetic beads were washed 5 times with the binding buffer to remove unbound DNA. Thereafter, 300 mM metronidazole was added and the mixture was gently shaken for another 2 h at room temperature, followed by the magnetic separation. The supernatant was collected, and its fluorescence intensity was determined. The pooled ssDNA in the supernatant was amplified by PCR and put into the next round of selection. The

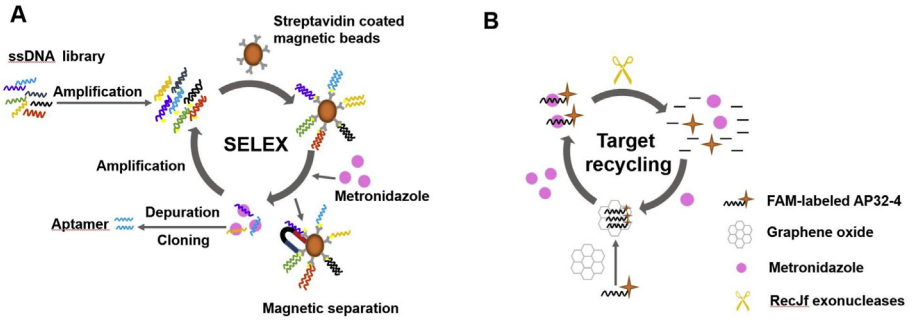


**Fig. 1.** (A) Schematic diagram of DNA library-immobilized SELEX. (B) Schematic illustration of target-recycling signal amplification for fluorescent detection of metronidazole.

SELEX was continuously conducted until the fluorescence intensity of the pooled supernatant reached saturation.

The ssDNA pooled at the last round of selection was amplified by PCR. The products were purified with gel recovery kit, then connected with pMD18-T vector and transferred into *Escherichia coli* JM109 for overnight culture. 39 positive clones were selected and sequenced by Sangon Biotechnology Co., Ltd. (Shanghai, China).

### 2.2. Sequence analysis and molecular docking

The primary structures and spatial structures of the selected aptamers were characterized and compared. The homology of these sequences was analyzed by DNAMAN and Snap Gene. The secondary structures of the aptamers were simulated and analyzed by RNA Structure software and online software Mfold Web Server. Then PyMoL 1.7.6 software was used to simulate the tertiary structures of the aptamers, and the 3D structure of metronidazole was got from the website Pubchem Project. And the molecular docking software Auto Dock Tools 1.5.6 was used to conduct molecular docking between the aptamer and metronidazole. Finally, the results of molecular docking were analyzed by PyMoL 1.7.6 software.

### 2.3. Characterization of the selected aptamers

To measure the dissociation constant ($K_d$) of the selected aptamers, different volume of the synthesized 5′-FAM labeled aptamer sequences were supplemented up to 200 μL with the binding buffer to prepare different concentration of the aptamers. Then the aptamer solution was denatured at 90 °C for 10 min, rapidly put in ice bath for 10 min, and placed at room temperature for 10 min. GO was added to the aptamer solution and the mixture was incubated for 2 h at room temperature to allow the adsorption of the aptamer onto GO. Then 1 μM metronidazole was added to the mixture, followed by slight shaking and displacement for 2 h at room temperature. After that, the mixture was centrifuged for 5 min at 13 000 r/min and supernatant was pooled. Finally, the supernatant was added into 96-well plate and the fluorescence intensity was measured with a microplate reader (emission wavelength: 520 nm, excitation wavelength: 494 nm). The content of the free aptamer in the supernatant is proportional to the fluorescence intensity. The $K_d$ values of the aptamers can be calculated through non-linear regression according to the equation $y = Bmax \times [free\ ssDNA]/(K_d+[free\ ssDNA])$. In the equation, y represents the proportion of metronidazole bound to aptamer to the total metronidazole, that is, saturation. Bmax represents the number of the maximum binding sites. And [free ssDNA] represents the concentration of free ssDNA that is not bound to metronidazole.

To evaluate the specificity of the aptamer for metronidazole, 200 μL of 500 mM FAM-labeled aptamer dissolved in the binding buffer was denatured at 90 °C for 10 min, rapidly put in ice bath for 10 min, and kept at room temperature for 10 min. Then, 80 μL of 5 mg/mL GO was added and incubated at room temperature for 2 h. Next, 1 μM different kinds of antibiotics were added to the mixture respectively. The mixture was incubated for 2 h at room temperature with gentle shaking, follow by centrifugation at 13 000 r/min for 5 min. The supernatant from different samples was added into 96-well plate and the fluorescence intensity was measured and compared to that of the sample with metronidazole.

### 2.4. Construction of fluorescent signal amplification sensor

The truncated optimal aptamer was utilized to construct a fluorescent biosensor for metronidazole to verify its practicability. The truncated aptamer was labeled with FAM at its 5′-end. GO was then introduced, which can not only adsorb aptamer *via* hydrophobic and π-π stacking interactions between the nucleobases of ssDNA and GO, but also quench the fluorescent signal of FAM modified on the aptamer. In the presence of metronidazole, the aptamer was competitively displaced from GO and formed aptamer/metronidazole complex in the solution. Then the fluorescent signal of FAM was recovered. Furthermore, the desorbed aptamer in the complex can be hydrolyzed by RecJf exonuclease,

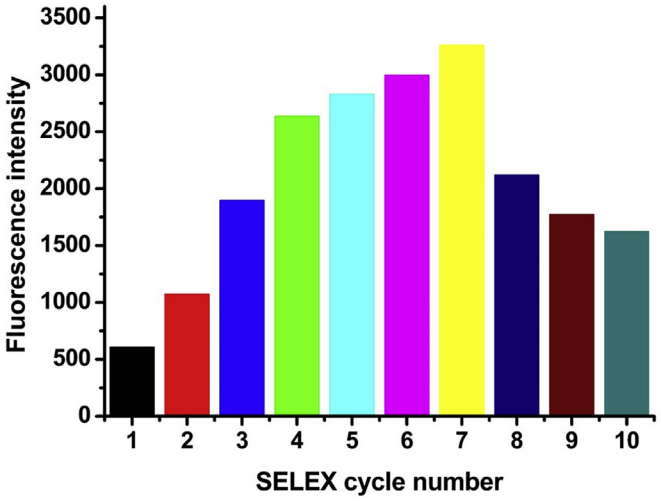


**Fig. 2.** Fluorescence intensity of the displaced ssDNA in the solution in each round of selection.

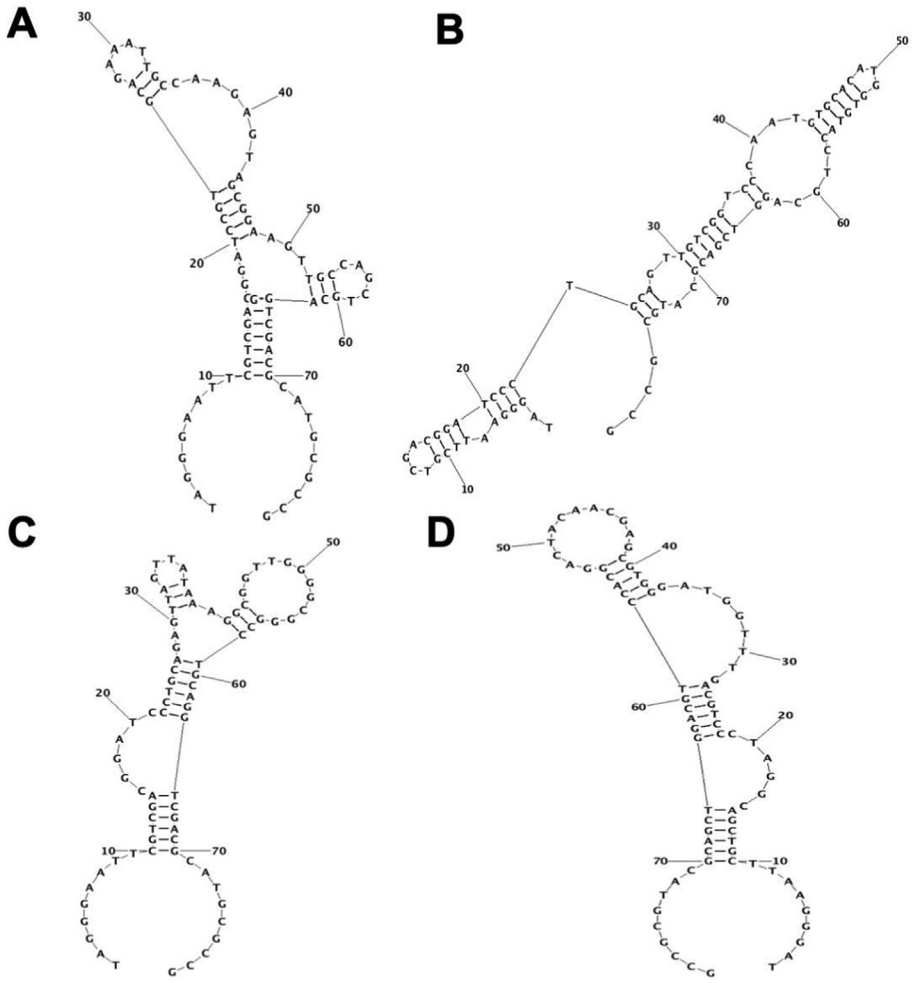


**Fig. 3.** The secondary structures of four selected aptamers. (A) AP2; (B) AP19; (C) AP21; (D) AP32.

releasing free metronidazole for target-recycling. Thus the amplification of the fluorescent signal can be achieved (Fig. 1B).

The truncated aptamer was diluted with binding buffer to the final concentration of 20 nM. 1 mL of 20 nM aptamer was mixed with 160 μL of 5 mg/mL GO and allowed to settle for 100 min. Then different concentrations of metronidazole were added to 200 μL of the above aptamer-GO mixture and incubated at 37 °C for 90 min. Thereafter 1 μL of 300 U/mL RecJf was added and incubated at 37 °C for 90 min, followed by centrifugation at 13 000 r/min for 5 min. Afterwards, the fluorescence spectra of the supernatant were collected with the excitation of 494 nm and the emission intensity at 520 nm was taken for quantitative analysis.

To verify the practicability, the assay was applied to detect metronidazole in artificially contaminated honey samples. To prepare honey samples, different concentrations of standard metronidazole solution were spiked to the 5-fold diluted honey samples. Then the detection was carried out according to the steps described above.

## 3. Results and discussion

### 3.1. In vitro selection of the aptamers

During the DNA library-immobilized SELEX, PCR products of ssDNA library was immobilized on magnetic beads in form of dsDNA, and sequences with high affinity for metronidazole were rehybridized with its complementary sequences and released into the solution in form of aptamer/metronidazole complex. The fluorescent signal of FAM labeled at the 5′-end of the aptamers was used to quantify the aptamers. The higher the fluorescence intensity is, the higher the affinity of ssDNA is in the solution toward metronidazole. As shown in Fig. 2, the fluorescence intensity continuously increases and reaches the maximum after seven rounds of selection. As the number of selection rounds increased, ssDNA with the higher affinity for metronidazole was gradually enriched, while ssDNA with comparatively low affinity was gradually eliminated. And then the selection reaches saturation. Nevertheless, three more selection rounds were performed to reduce possible false positive sequences, during which the fluorescence intensity decayed [37]. The pooled ssDNA in the tenth round of selection was PCR amplified and cloned for sequencing.

### 3.2. Characterization of the selected aptamers

After ten rounds of selection and enrichment, 39 positive clones were selected for sequencing. The obtained sequences are listed in Table S1 in Supporting information. These aptamers are classified into seven families according to their sequence homology. The homologous regions are highlighted. The representative aptamers are rich in conservative motifs “GGT” and “GTT” (shown in bold

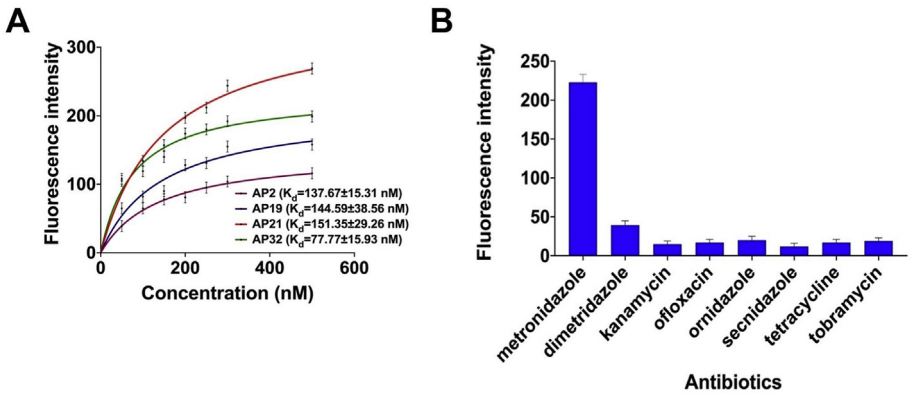


**Fig. 4.** (A) The saturation curves and $K_d$ values of AP2, AP19, AP21 and AP32. (B) Verification of the specificity of AP32 to metronidazole.

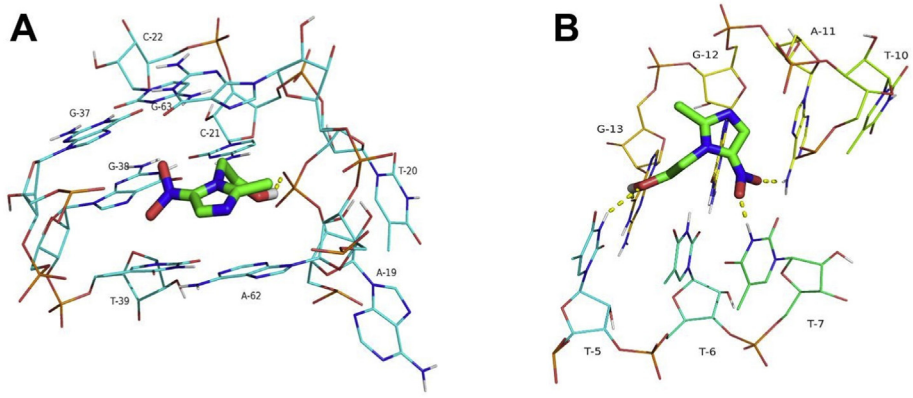


**Fig. 5.** (A) Molecular docking of AP32 and metronidazole; (B) Molecular docking of AP32-3 and metronidazole.

**Table 1**
Sequences and dissociation constant ($K_d$) values of the truncated aptamers.

| Aptamers | Sequences (5′-3′) | $K_d$ (nM) |
|---|---|---|
| AP32 | TAGGGAATTCGTCGACGGATCCCTGCAGTTTGGTAGGGTGCGAGCAACATCAGGCACCTGCAGGTCGACGCATGCGCCG | 77.77 ± 15.93 |
| AP32-1 | ATCCCTGCAGTTTGGTAGGGTGCGAGCAACATCAGGCACCTGCAGG | 41.05 ± 12.58 |
| AP32-2 | ATCCCTGCAGTTTGGTAGGGTGCAGG | 97.38 ± 29.00 |
| AP32-3 | CTGCTTTGGTAGGGCAG | 75.04 ± 22.30 |
| AP32-4 | CTGTTTGGTAGGCAG | 77.22 ± 11.27 |

letters), which may be important during the recognition and binding to the target. Among them, AP2, AP19, AP21 and AP32 were chosen for further characterization. Next, RNA Structure software is used to simulate and predict the secondary structures of the four aptamers, as shown in Fig. 3. In the secondary structure diagrams, the conservative motif "GGT" is usually located in the ring regions. These structural characteristics are likely related to the specific binding of the aptamers to metronidazole.

Then the dissociation constants ($K_d$) of the aptamers were determined to evaluate the affinity of these aptamers for metronidazole by fluorescence method. These aptamers were chemically synthesized and labeled with FAM at their 5′-end. GO was utilized to adsorb FAM-labeled aptamers and quench the fluorescent signal. On the contrary, metronidazole competitively bound to aptamers and released them from GO, subsequently recovered the fluorescent signal. To plot the saturation curve, a serial of different concentrations of the aptamers were used, whereas the concentration of metronidazole was fixed. Content of the aptamer was directly proportional to the fluorescence intensity. According to the equation $y = Bmax \times [free\ ssDNA]/(K_d+[free\ ssDNA])$ and nonlinear fitting by software GraphPad Prism 8.0, the dissociation constants of each aptamer can be determined (Fig. 4A). Among these aptamers, AP32 has the lowest $K_d$ value of 77.77 ± 15.93 nM, which means the highest affinity for metronidazole. Then, the specificity of AP32 was evaluated. Other antibiotics rather than metronidazole were used to displace AP32 from GO and the fluorescence intensity of the solution was measured. As shown in Fig. 4B, the fluorescence intensity obtained in the presence of metronidazole was much higher than those of other antibiotics. Dimetridazole, another nitroimidazole derivative, shows slight binding with AP32. The binding of antibiotics from other families can be neglected. This indicates high specificity of the aptamer.

### 3.3. Truncation of the aptamer

Truncation was carried out in a semi-rational mode, that is, truncation scheme is based on both structural prediction and affinity analysis. Molecular docking was firstly carried out to predict

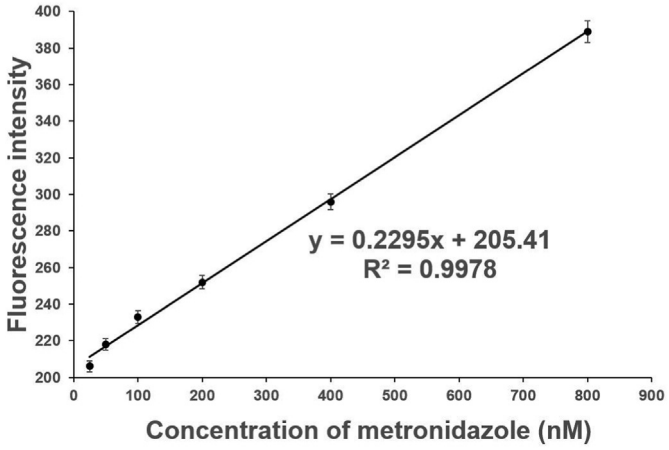


**Fig. 6.** The linear relationship between fluorescence intensity and the concentration of metronidazole in standard solution.

**Table 2**
Detection of metronidazole in 5-fold diluted honey samples.

| Samples | Added (nM) | Found (nM) | Recovery (%) | RSD (%) |
|---|---|---|---|---|
| Sample 1 | 200 | 196.5 | 98.25 | 5.08 |
| Sample 2 | 400 | 394.7 | 98.67 | 4.76 |
| Sample 3 | 600 | 612.6 | 102.10 | 3.92 |

the binding site of AP32 and metronidazole, and the energy-optimal conformation is selected during the docking. As shown in Fig. 5A, metronidazole is surrounded with the oligonucleotide chain of the aptamer, mainly through hydrophobic interaction and van der Waals force. The nucleotides located at the binding site include A19, T20, C21, C22, G37, G38, T39, A62 and G63. Then we optimized the structure of AP32 by step-removing of the extraneous nucleotides and comparing the affinity of the truncated aptamer to that of AP32. If the $K_d$ of the truncated aptamer is lower than 100 nM, the truncation scheme is retained; otherwise, the truncation scheme is abandoned. The ultimate goal is to obtain an aptamer with the shortest possible length and acceptable affinity.

First of all, a structurally stable truncated aptamer AP32-1 with the length of 46 nt was obtained by removing the stem-ring structure without binding site (Fig. S1). The affinity of AP32-1 for the target is apparently enhanced, which may be ascribed to the deletion of redundant sequence. However, the length of AP32-1 is still not satisfactory for real application. Thus multiple truncation attempts were subsequently conducted on the basis of AP32-1, and finally a feasible scheme to truncate the aptamer to 17 nt was found, resulting in the aptamer AP32-3. Although the $K_d$ values of the gradually shortened aptamers experience fluctuation, the affinity maintains in the acceptable range. The sequences and $K_d$ of the truncated aptamers are listed in Table 1. Molecular docking of AP32-3 and metronidazole shows that compared with the original aptamer, the binding site of the truncated aptamer is most likely to be at the junction of the stem and the loop structure (Fig. 5B). Furthermore, by considering the predicted binding site and comparing the affinity of various 15 nt-length sequences, a truncated aptamer AP32-4 was finally obtained, whose $K_d$ is determined to be 77.22 ± 11.27 nM. To sum up, according to the secondary structure analysis and binding site prediction, the aptamer was truncated through step-removing of the stem-loop structure and other regions without the binding site. During the truncation, we found that the binding site of the aptamer shifts, which may be ascribed to the conformational change of the oligonucleotides. Nevertheless, the binding site generally distributes at the critical region of stem-loop structure. Upon the deletion of redundant sequence, the length of the aptamer reaches the minimum, while the $K_d$ value of AP32-4 is almost equivalent to that of AP32. Thus, the screened optimal aptamer laid a solid basis for further application in the construction of biosensors for metronidazole.

### *3.4. Detection of metronidazole based on truncated AP32-4 and target-recycling fluorescent signal amplification*

To evaluate the performance of the screened aptamer in practical application, a simple fluorescent biosensor for metronidazole was constructed with a target-recycling signal amplification unit. GO was employed to adsorb FAM-labeled AP32-4 and quench the fluorescent signal of FAM. Metronidazole can recover the fluorescent signal through displace the aptamer from GO, while RecJf exonuclease was used to hydrolyze the aptamer and release metronidazole for target-recycling and fluorescent signal amplification. After the addition of RecJf exonuclease, the aptamer is hydrolyzed and no band can be observed. The same phenomenon appears when GO is introduced. Since the aptamer is adsorbed on the surface of GO, no aptamer exists in the solution. Nevertheless, when AP32-4, GO and metronidazole are co-existence, the band represents AP32-4 can be observed, which means AP32-4 exists in the solution. However, upon the addition of RecJf exonuclease to the mixture of AP32-4, GO and metronidazole, the band disappears once again, indicating the hydrolysis of the aptamer. These results prove that GO can effectively adsorb the aptamer, while metronidazole can release aptamer, which can be further hydrolyzed by RecJf exonuclease.

In order to obtain the best performance, several reaction conditions of the fluorescent signal amplification sensor were optimized, including the concentration of the aptamer, the amount of RecJf exonuclease, the incubation time and temperature. Fluorescence intensity was used as the index during the experimental optimization. With the increase of the concentration of AP32-4, the fluorescence intensity increases and then keeps constant when AP32-4 is higher than 2 μM (Fig. S2A). The increase of the amount of RecJf exonuclease can accelerate the hydrolysis of the released aptamer and the recycling of metronidazole. The fluorescence intensity reaches the maximum when 1.5 U RecJf exonuclease is added (Fig. S2B). The incubation time and temperature can greatly influence the hydrolytic reaction of RecJf exonuclease and thus were optimized. The highest fluorescence intensity is detected when 90 min and 37 °C are employed (Figs. S2C and S2D).

Under the optimal conditions, the relationship between the fluorescence intensity of the biosensor and the concentration of metronidazole was studied. The results are shown in Fig. 6. Fluorescence intensity gradually increases with the increased concentration of metronidazole in the samples. A good linear relationship between the fluorescence intensity and metronidazole concentration can be derived in the range of 25–800 nM. The linear regression equation is $y = 0.2295x+205.41$ ($R^2 = 0.9978$), where y represents the fluorescence intensity, and x represents the concentration of metronidazole (nM). The detection limit of the sensor is estimated to be 10.50 nM. According to the technical recommendations of the analytical method given by the European Reference Laboratory (EURL), the detection concentration of metronidazole is 3 μg/kg (approximately 24.53 nM). Thus the developed assay can meet the detection requirement of metronidazole residue.

In order to develop the application potential of the truncated aptamer-based biosensor in practical sample detection, the target recycling sensor was applied to detect metronidazole in artificially

contaminated honey. The detection was repeated for 3 times at each concentration. The results are listed in Table 2. The recovery rate of metronidazole in honey samples is in the range of 98.25–102.1%, and the relative standard deviation (RSD) is within 3.92–5.08%. The results indicate excellent performance of the biosensor in detection of honey samples.

## 4. Conclusions

In summary, overall 39 metronidazole-specific aptamer sequences were firstly selected based on DNA library-immobilized magnetic beads SELEX technology from an initial library containing 35 random oligonucleotides with a total length of 79 nt through 10 rounds of selection. After the classification of these aptamers, four sequences with highly similar secondary structures were picked up for affinity evaluation, among which the one with the lowest $K_d$, AP32 was chosen as the optimal original sequence for post-SELEX truncation. The truncation was conducted under a semi-rational fashion based on both structural prediction and multiple trial followed by affinity evaluation. A truncated aptamer with the length of only 15 nt, AP32-4 was eventually obtained, without the loss of affinity. The selection and truncation methods used in this work may provide an efficient and universal strategy for the screening of robust, low-cost and high affinity aptamers for diverse targets. To investigate the practicability of the truncated aptamer, it was used to construct an aptamer-based fluorescent biosensor based on target-recycling signal amplification, which was applied to detect both standard metronidazole solution and the actual honey samples. The high sensitivity and satisfactory recovery and RSD in real samples suggest the application prospect of the biosensor in food safety, environment monitoring and medical analysis.

## CRediT authorship contribution statement

**Hao Wei:** Conceptualization, Methodology, Software, Writing - original draft. **Rongfeng Cai:** Software, Validation. **Hui Yue:** Visualization, Investigation. **Yaping Tian:** Supervision. **Nandi Zhou:** Writing - review & editing, Supervision.

## Declaration of competing interest

The authors declare that they have no known competing financial interests or personal relationships that could have appeared to influence the work reported in this paper.

## Acknowledgments

This work was supported by the Six Talent Peaks Project in Jiangsu Province (JY-078) and the National Natural Science Foundation of China (no. 31271860).

## Appendix A. Supplementary data

Supplementary data to this article can be found online at https://doi.org/10.1016/j.aca.2020.07.003.

## References

[1] L. Kumar, A. Jain, N. Lal, A. Sarswat, S. Jangir, L. Kumar, V. Singh, P. Shah, S.K. Jain, J.P. Maikhuri, M.I. Siddiqi, G. Gupta, V.L. Sharma, Potentiating metronidazole scaffold against resistant trichomonas: design, synthesis, biology and 3d-QSAR analysis, ACS Med. Chem. Lett. 3 (2012) 83–87.
[2] A.M. Jarrad, T. Karoli, A. Debnath, C.Y. Tay, J.X. Huang, G. Kaeslin, A.G. Elliott, Y. Miyamoto, S. Ramu, A.M. Kavanagh, J. Zuegg, L. Eckmann, M.A.T. Blaskovich, M.A. Cooper, Metronidazole-triazole conjugates: activity against clostridium difficile and parasites, Eur. J. Med. Chem. 101 (2015) 96–102.
[3] M. Liu, X.-Y. Li, J.-J. Li, X.-M. Su, Z.-Y. Wu, P.-F. Li, F.-H. Lei, X.-C. Tan, Z.-W. Shi, Synthesis of magnetic molecularly imprinted polymers for the selective separation and determination of metronidazole in cosmetic samples, Anal. Bioanal. Chem. 407 (2015) 3875–3880.
[4] M.P. Prabhakaran, M. Zamani, B. Felice, S. Ramakrishna, Electrospraying technique for the fabrication of metronidazole contained PLGA particles and their release profile, Mater. Sci. Eng. C 56 (2015) 66–73.
[5] M.R. El-Ghobashy, N.F. Abo-Talib, Spectrophotometric methods for the simultaneous determination of binary mixture of metronidazole and diloxanide furoate without prior separation, J. Adv. Res. 1 (2010) 323–329.
[6] H. Pan, W. Ba-Thein, Diagnostic accuracy of global pharma health fund minilab™ in assessing pharmacopoeial quality of antimicrobials, Am. J. Trop. Med. Hyg. 98 (2018) 344–348.
[7] A. Hatamie, F. Marahel, A. Sharifat, Green synthesis of graphitic carbon nitride nanosheet (g-$C_3N_4$) and using it as a label-free fluorosensor for detection of metronidazole via quenching of the fluorescence, Talanta 176 (2018) 518–525.
[8] X.Y. Hu, J. Fan, K.L. Zhang, N. Yu, J.J. Wang, Pharmaceuticals removal by novel nanoscale photocatalyst $Bi_4VO_8Cl$: influencing factors, kinetics, and mechanism, Ind. Eng. Chem. Res. 53 (2014) 14623–14632.
[9] C. Ho, D.W.M. Sin, K.M. Wong, H.P.O. Tang, Determination of dimetridazole and metronidazole in poultry and porcine tissues by gas chromatography-electron capture negative ionization mass spectrometry, Anal. Chim. Acta 530 (2005) 23–31.
[10] M.T. Jafari, B. Rezaei, B. Zaker, Ion mobility spectrometry as a detector for molecular imprinted polymer separation and metronidazole determination in pharmaceutical and human serum samples, Anal. Chem. 81 (2009) 3585–3591, https://doi.org/10.1021/ac802557t. https://search.crossref.org/?q=Ion+mobility+spectrometry+as+a+detector+for+molecular+imprinted+polymer+separation+and+metronidazole+determination+in+pharmaceutical+and+human+serum+samples.
[11] N. Xiao, J. Deng, J.L. Cheng, S.Q. Ju, H.Q. Zhao, J. Xie, D. Qian, J. He, Carbon paste electrode modified with duplex molecularly imprinted polymer hybrid film for metronidazole detection, Biosens. Bioelectron. 81 (2016) 54–60.
[12] C.C. Chen, J.X. Luo, C.L. Li, M.F. Ma, W.B. Yu, J.Z. Shen, Z.H. Wang, Molecularly imprinted polymer as an antibody substitution in pseudo-immunoassays for chemical contaminants in food and environmental samples, J. Agric. Food Chem. 66 (2018) 2561–2571.
[13] V. Velusamy, S. Palanisamy, T. Kokulnathan, S.-W. Chen, T.C.K. Yang, C.E. Banks, S.K. Pramanik, Novel electrochemical synthesis of copper oxide nanoparticles decorated graphene-β-cyclodextrin composite for trace-level detection of antibiotic drug metronidazole, J. Colloid Interface Sci. 530 (2018) 37–45.
[14] C.S. Thompson, I.M. Traynor, T.L. Fodey, S.R.H. Crooks, Improved screening method for the detection of a range of nitroimidazoles in various matrices by optical biosensor, Anal. Chim. Acta 637 (2009) 259–264.
[15] M. Berezovski, A. Drabovich, S.M. Krylova, M. Musheev, V. Okhonin, A. Petrov, S.N. Krylov, Nonequilibrium capillary electrophoresis of equilibrium mixtures: a universal tool for development of aptamers, J. Am. Chem. Soc. 127 (2009) 3165–3171.
[16] J.W. Park, R. Tatavarty, D. Kim, H.-T. Jung, M.B. Gu, Immobilization-free screening of aptamers assisted by graphene oxide, Chem. Commun. 48 (2012) 2071–2073.
[17] V.-T. Nguyen, Y.S. Kwon, J.H. Kim, M.B. Gu, Multiple GO-SELEX for efficient screening of flexible aptamers, Chem. Commun. 50 (2014) 10513–10516.
[18] F.M. Spiga, F. Maietta, C. Guiducci, More DNA–aptamers for small drugs: a capture-SELEX coupled with surface plasmon resonance and high-throughput sequencing, ACS Comb. Sci. 17 (2015) 326–333.
[19] N. Qiao, J. Li, X. Wu, D.L. Diao, J.X. Zhao, J.Y. Li, X.J. Ren, X.F. Ding, D.H. Shangguan, X.H. Lou, Speeding up in vitro discovery of structure-switching aptamers via magnetic cross-linking precipitation, Anal. Chem. 91 (2019) 13383–13389.
[20] Y. Luo, J. Wang, L.Y. Yang, T. Gao, R.J. Pei, In vitro selection of DNA aptamers for the development of fluorescent aptasensor for sarcosine detection, Sensor. Actuator. B Chem. 276 (2018) 128–135.
[21] N.D. Zhou, J.Y. Wang, J. Zhang, C. Li, Y.P. Tian, J. Wang, Selection and identification of streptomycin-specific single-stranded DNA aptamers and the application in the detection of streptomycin in honey, Talanta 108 (2013) 109–116.
[22] X.Y. Han, Y.H. Zhang, J.J. Nie, S.Y. Zhao, Y.P. Tian, N.D. Zhou, Gold nanoparticle based photometric determination of tobramycin by using new specific DNA aptamers, Microchim. Acta 185 (2018) 4.
[23] Y. Yang, D.L. Yang, H.J. Schluesener, Z.R. Zhang, Advances in SELEX and application of aptamers in the central nervous system, Biomol. Eng. 24 (2007) 583–592.
[24] J. Macdonald, P. Houghton, D.X. Xiang, W. Duan, S. Shigdar, Truncation and mutation of a transferrin receptor aptamer enhance binding affinity, Nucleic Acid Therapeut. 26 (2016) 348–354.
[25] L.-L. Yang, X. Yang, G.-B. Li, K.-G. Fan, P.-F. Yin, X.-G. Chen, An integrated molecular docking and rescoring method for predicting the sensitivity spectrum of various serine hydrolases to organophosphorus pesticides, J. Sci. Food Agric. 96 (2016) 2184–2192.
[26] Y. Yang, X. Ren, H.J. Schluesener, Z. Zhang, Aptamers: selection, modification and application to nervous system diseases, Curr. Med. Chem. 18 (2011)

4159–4168.
[27] E. Ouellet, E.T. Lagally, K.C. Cheung, C.A. Haynes, A simple method for eliminating fixed-region interference of aptamer binding during SELEX, Biotechnol. Bioeng. 111 (2014) 2265–2279.
[28] Z.W. Wang, H.X. Yu, J. Canoura, Y.Z. Liu, O. Alkhamis, F.F. Fu, Y. Xiao, Introducing structure-switching functionality into small-molecule-binding aptamers via nuclease-directed truncation, Nucleic Acids Res. 46 (2018) e81.
[29] Y.Y. Zhu, Y.L. Cai, L.G. Xu, L.X. Zheng, L.M. Wang, B. Qi, C.L. Xu, Building an aptamer/graphene oxide FRET biosensor for one-step detection of bisphenol A, ACS Appl. Mater. Interfaces 7 (2015) 7492–7496.
[30] M.K. Wang, Z.H. Lin, Q. Liu, S. Jiang, H. Liu, X.G. Sun, DNA-hosted copper nanoclusters/graphene oxide based fluorescent biosensor for protein kinase activity detection, Anal. Chim. Acta 1012 (2018) 66–73.
[31] Z.J. Huang, Z.W. Luo, J.M. Chen, Y. Xu, Y.X. Duan, A facile, label-free, and universal biosensor platform based on target-induced graphene oxide constrained DNA dissociation coupling with improved strand displacement amplification, ACS Sens. 3 (2018) 2423–2431.
[32] H.J. Gu, N. Duan, Y. Xia, X. Hun, H.T. Wang, Z.P. Wang, Magnetic separation-based multiple SELEX for effectively selecting aptamers against saxitoxin, domoic acid, and tetrodotoxin, J. Agric. Food Chem. 66 (2018) 9801–9809.
[33] X.-M. Shi, G.-C. Fan, Q. Shen, J.-J. Zhu, Photoelectrochemical DNA biosensor based on dual-signal amplification strategy integrating inorganic-organic nanocomposites sensitization with λ-exonuclease-assisted target recycling, ACS Appl. Mater. Interfaces 8 (2016) 35091–35098.
[34] A.-L. Sun, Y.-F. Zhang, G.-P. Sun, X.-N. Wang, T.P. Tang, Homogeneous electrochemical detection of ochratoxin A in foodstuff using aptamer–graphene oxide nanosheets and DNase I-based target recycling reaction, Biosens. Bioelectron. 89 (2017) 659–665.
[35] H. Rezaeia, M. Motovali-bashia, S. Radfarb, An enzyme-free electrochemical biosensor for simultaneous detection of two hemophilia A biomarkers: combining target recycling with quantum dots-encapsulated metal-organic frameworks for signal amplification, Anal. Chim. Acta 1092 (2019) 66–74.
[36] X.L. Zhang, Z.H. Yang, Y.Y. Chang, M. Qing, R. Yuan, Y.Q. Chai, A novel 2D DNA nanoprobe mediated enzyme-free target recycling amplification for ultrasensitive electrochemical detection of microRNA, Anal. Chem. 90 (2018) 9538–9544.
[37] S. Valenzano, A.D. Girolamo, M.C. DeRosa, M. McKeague, R. Schena, L. Catucci, M. Pascale, Screening and identification of DNA aptamers to tyramine using in vitro selection and high-throughput sequencing, ACS Comb. Sci. 18 (2016) 302–313.